ACS APPLIED MATERIALS & INTERFACES

www.acsami.org

Research Article

Magnetic ZIF-8-Based Mimic Multi-enzyme System as a Colorimetric Biosensor for Detection of Aryloxyphenoxypropionate Herbicides

Hengyan Ma, Mengya Li, Ting Yu, Hui Zhang,* Minghua Xiong, and Feng Li*

Cite This: *ACS Appl. Mater. Interfaces* 2021, 13, 44329–44338

Read Online

ACCESS | Metrics & More | Article Recommendations | Supporting Information

ABSTRACT: In the present study, a magnetic mimic multi-enzyme system was developed by encapsulating the aryloxyphenoxypropionate (AOPP) herbicide hydrolase QpeH and alcohol oxidase (AOx) in zeolitic imidazolate framework (ZIF-8) nanocrystals with magnetic Fe_3O_4 nanoparticles (MNPs) to detect AOPP herbicides. The structural, protein loading capacity and loading ratio, porosity, and magnetic properties of QpeH/AOx@mZIF-8 were characterized by scanning electron microscopy, X-ray diffraction, Fourier transform infrared spectroscopy, thermogravimetric analysis, nitrogen sorption, and vibrating sample magnetometry. An AOPP herbicide colorimetric biosensor made with QpeH/AOx@mZIF-8 had the highest sensitivity toward quizalofop-P-ethyl (QpE) with a limit of detection of 8.2 μM. This system was suitable to detect two other AOPP herbicides, including fenoxaprop-P-ethyl (FpE) and haloxyfop-P-methyl (HpE). The practical application of the biosensor was verified through quantitative analysis of QpE residues in industrial wastewater and field soils. Furthermore, QpeH/AOx@mZIF-8 exhibited excellent long-term storage stability (at least 50 days), easy separation by magnet, and reusability (at least 10 cycles), supporting its promising role in simple and low-cost detection of AOPP herbicides in real environmental samples.

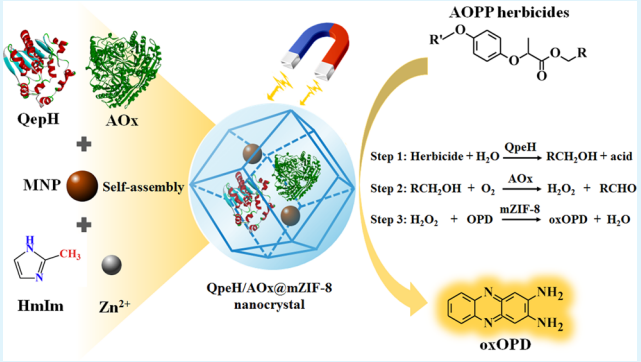

KEYWORDS: *aryloxyphenoxypropionate herbicides, magnetic nanoparticle, ZIF-8, colorimetric biosensor, detection*

INTRODUCTION

Aryloxyphenoxypropionate (AOPP) herbicides are primarily used as selective post-emergence herbicides to control annual and perennial grass weeds in different broadleaf crops.[1] AOPP herbicides have been commercially manufactured and applied in more than 100 countries worldwide since their discovery in the mid-1940s.[2] In 2014, the world AOPP herbicide expenditure reached approximately $12.17 billion, accounting for 4.6% of the global herbicide market.[3] The new herbicide market analysis has projected to the global herbicide sales to increase by 2022.[4] The increasing crop yield has optionally contributed to large quantities of AOPP herbicides into the environment, leading to severe contamination of groundwater and distant surface water systems.[5] AOPP herbicides and their metabolites are abundant in natural water, soil, vegetables, and fruits due to their extensive use, water solubility, and relatively high mobility.[6] Toxicological data demonstrated that low doses of AOPP herbicides (100 μM) and frequent exposure even in trace levels could induce DNA damage of non-target organisms[7] and liver and lung injury in rats and humans, respectively.[8,9] Except for the adverse impacts, AOPP herbicide residues are also detrimental to rotation crops, leading to high food safety risks.[10] Therefore, establishing a routine monitoring system with high sensitivity, specificity, and reliability is highly necessitated to rapidly determine the AOPP herbicide residue concentration in the environment.

Currently, AOPP herbicide detection is highly dependent on the sensitivity and reliability of sophisticated instrumentations, such as UV−vis absorption, high-performance liquid chromatography−tandem mass spectrometry (HPLC−MS), and gas chromatography−tandem mass spectrometry (GC−MS).[11,12] However, these methods are time-consuming, expensive, and complicated in terms of sample pre-preparation and trained technicians. The enzyme-based electrochemical biosensors have emerged as revolutionary strategies meeting the need for rapid, low-cost, reliable, and one-site analysis of AOPP herbicide residues in complex environmental samples.[13] Generally, four types of biomolecules, including DNA, antibodies or antigens, aptamer, and enzyme molecules, are used in the electrochemical biosensors for analyte recognition. Nevertheless, the DNA sensors, immunosensors, and aptasen-

Received: June 24, 2021
Published: September 8, 2021

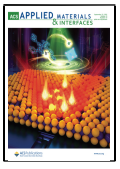

https://doi.org/10.1021/acsami.1c11815
ACS Appl. Mater. Interfaces 2021, 13, 44329−44338

Scheme 1. Schematic Illustration of the One-Pot Synthesis of QpeH/AOx@mZIF Composite with Magnetic Collection and Utilized as a Biosensor for the Rapid Detection of AOPP Herbicides

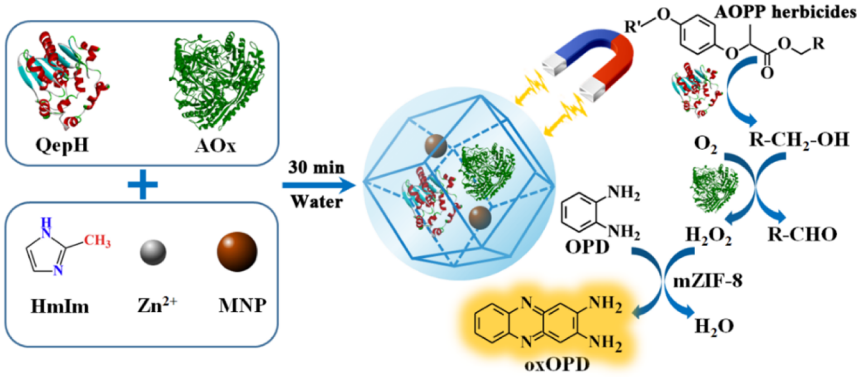

sors are reported to exert several demerits, such as low selectivity,[14] low stability,[15] and fabrication difficulty.[16] Recently, the enzyme-based biosensors have gained increasing attention in pesticide detection due to their high activity and selectivity under ambient conditions.

In enzyme-based biosensors, the enzyme molecules are usually immobilized in the working electrode by a variety of methods for ease of operation. However, practical applications of natural enzymes are often hampered by the limitations of low chemical and storage stability, high cost, and difficult recovery and reusability.[17] In this regard, enzyme immobilization could be an alternative to overcome these challenges during the immobilization method, nanotechnology, and fabrication process. Metal−organic frameworks (MOFs), the self-assembled metal ions and organic ligands, are the novel hybrid crystalline nanomaterials. The MOF-supporting enzyme immobilization possesses several unique properties, such as tunable porosity, large surface areas, and post-synthetic modifiability due to its diverse topological architecture. These characteristics help to improve the loading capacity, enzyme activity, and stability against adverse conditions.[18] Accumulating studies have reported various biosensors using MOFs as a support platform for monitoring pesticides.[19,20] However, the analysis of most pollutants cannot be achieved by one-step assay and requires a multi-enzyme system equipped with a series of consecutive proceeding cascade reactions. A recent study has reported rapid multi-enzyme co-immobilization through biomimetic mineralization procedures.[21] In this process, the negatively charged enzyme molecules in the aqueous solution bind with MOF precursors and act as the nucleation center for MOF crystal formation.[22] In a previous study, two model enzymes, glucose oxidase (GOx) and horseradish peroxidase (HRP), were encapsulated successfully into a zeolitic imidazolate framework (ZIF-8) to form multiple enzyme-embedded composites for glucose detection.[21] It is worth mentioning that high dispersity and low density result in difficult recovery and reusability of MOFs. Therefore, magnetic Fe_3O_4 nanoparticles (MNPs) are incorporated as seeds to prepare magnetic MOF composites (mMOFs), defined as a "nanozyme". These mMOFs exhibit mimetic peroxidase activity.[23] In recent years, nanozymes have been widely explored for biomolecule sensing due to their excellent robustness, simplicity, and cost-effective characteristics.[24] Hou *et al.* utilized embedded GOx and mimetic peroxidase of magnetic ZIF-8 (mZIF-8) to develop a mimic multi-enzyme system mZIF-8@GOx as a colorimetric biosensor for detecting glucose. This model exhibited a linear correlation at low concentration.[25] Ricco *et al.* developed an HRP/MNP@ZIF-8 composite in a one-pot synthesis without adding the compatibilizing agents for detecting the pyrogallol through H_2O_2-mediated oxidation.[26] To the best of our knowledge, one catalytic reaction is insufficient to detect most of the herbicides, especially AOPP herbicides. Therefore, the development of an enzyme-based biosensor for rapid quantitative analysis of these target pollutants is still unexplored.

Herein, a facile one-pot synthesis was introduced to develop a mimic multi-enzyme system based on mZIF-8 simultaneously encapsulating the AOPP herbicide hydrolase QpeH and alcohol oxidase (AOx) in an aqueous solution (Scheme 1). In this system, a three-step cascade reaction was completed orderly in a single magnetic nanoparticle QpeH/AOx@mZIF-8 and achieved rapid detection of AOPP herbicides through the naked eye in the lower concentration range, evading the diffusion hindrance and decomposition of intermediates as well as the cumbersome washing procedures such as ELISA. The fabricated QpeH/AOx@mZIF-8 composite initially catalyzed the hydrolysis of AOPP herbicides by embedded QpeH to form the corresponding acids and alcohol and subsequently oxidized the latter by an embedded second enzyme AOx to produce H_2O_2. The peroxidase-like activity of mZIF-8 then immediately catalyzed the oxidation of *o*-phenylenediamine (OPD) in the presence of H_2O_2 to form an orange-colored product 2,3-diaminophenazine (DAP). QpeH/AOx@mZIF-8 exhibited excellent analytical performances, such as low detection limit, wide detection spectrum, high enzymatic activity and storage stability, and ease of recycling for sensing AOPP herbicides in environmental samples.

EXPERIMENTAL SECTION

Materials. AOPP herbicides, $FeCl_3{\cdot}6H_2O$, $FeSO_4{\cdot}7H_2O$, 2-methylimidazole (HmIm), $Zn(NO_3)_2{\cdot}6H_20$, and *o*-phenylenediamine (OPD) were obtained from Aladdin Industrial Inc., China. Trisodium citrate dihydrate ($C_6H_5O_7Na_3{\cdot}2H_2O$), ammonia solution (25%), H_2O_2 (30%), ethanol, and other chemicals and solvents were purchased from Shanghai Chemical Reagent Co., Ltd (China). All the above chemicals used in this study were of analytical grade. The AOPP herbicide hydrolase QpeH from *Pseudomonas* sp. J-2 was expressed in *Escherichia coli* cells and purified by Ni^{2+} affinity chromatography.[27] Alcohol oxidase (AOx) from *Pichia pastoris* was procured from Beijing Solarbio Science & Technology Co., Ltd (China).

https://doi.org/10.1021/acsami.1c11815
ACS Appl. Mater. Interfaces 2021, 13, 44329−44338

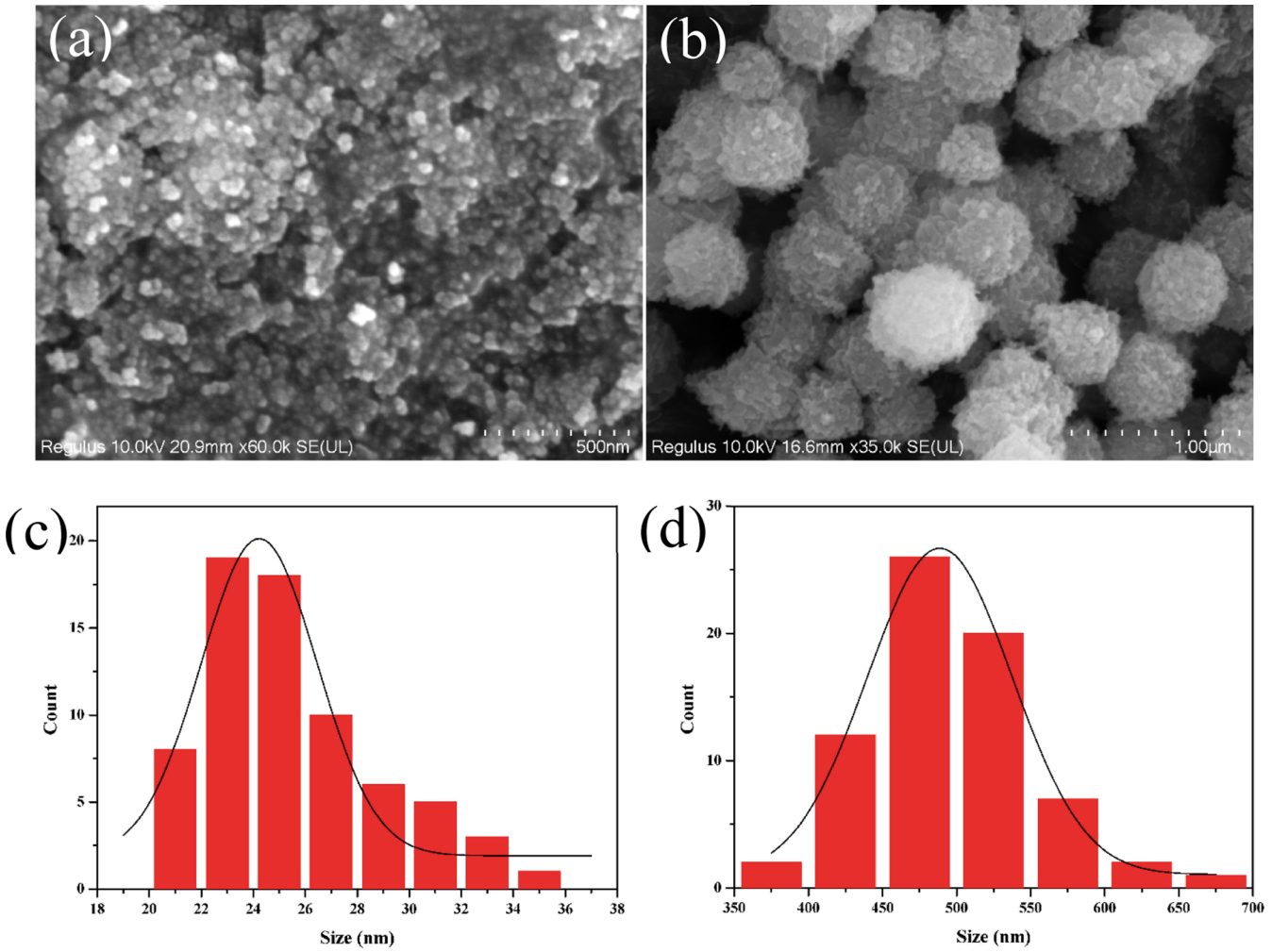

Figure 1. SEM images of (a) CA-Fe_3O_4 MNPs and (b) QpeH/AOx@mZIF-8 composite and size distributions of (c) CA-Fe_3O_4 MNPs and (d) QpeH/AOx@mZIF-8 composites.

Preparation of Fe_3O_4 MNPs. The citric acid coated Fe_3O_4 (CA-Fe_3O_4) MNPs were prepared *via* co-precipitation of Fe(III) and Fe(II) ions.[28] Briefly, 3.25 g of $FeCl_3{\cdot}6H_2O$ and 1.67 g of $FeSO_4{\cdot}7H_2O$ were dissolved in 50 mL of deionized (DI) water under vigorous stirring at 50 °C for 30 min. After complete dissolution, the mixture was heated to 75 °C, and ammonia solution (6.25 mL, 25% w/w) was added dropwise under continuous stirring for 60 min. Later, 1.5 M of trisodium citrate (6.25 mL) was added and stirred continuously for another 90 min at 85 °C under N_2 and allowed to cool at room temperature. Afterward, the black precipitate was separated by immersing a strong magnet into the solution for 5 min. The resulting product was washed thrice with DI water and ethanol and finally dried in a vacuum oven at 60 °C for 6 h.

Synthesis of mZIF-8 and QpeH/AOx@mZIF-8. mZIF-8 and QpeH/AOx@mZIF-8 composite were synthesized according to the method described by He *et al.*[29] CA-Fe_3O_4 MNPs (20 mg) were suspended in 2 mL of DI water and sonicated for 15 min to ensure homogeneous dispersion. The MNP suspension was then mixed with $Zn(NO_3)_2$ solution (0.4 M, 1 mL) and HmIm solution (1.25 M, 10 mL) under stirring for 30 min at room temperature. The mixture was centrifuged at 6,000 g for 10 min, and the precipitate was washed thrice with DI water. The final products were freeze-dried overnight to determine the yield. The same procedure was followed for QpeH/AOx@mZIF-8 or AOx@mZIF-8 composite synthesis, only using QpeH (15 mg mL^{-1}) and AOx (5 mg mL^{-1}) solution or AOx (5 mg/mL) solution instead of an equal volume of DI water. The pure ZIF-8 was also synthesized without the addition of MNPs and enzymes.

Characterization Methods. The morphologies of the samples were characterized by field-emission scanning electron microscopy (SEM, HITACHI Regulus 8220) equipped with energy-dispersive X-ray spectrometry (EDS) and Fourier transform infrared (FT-IR) spectroscopy (Thermo Nicolet 4700). The crystal structures of the samples were recorded with powder X-ray diffraction (XRD, Bruker D8 Advance) within the range of 2θ between 5 and 50°. The magnetic properties at room temperature were measured by a vibrating sample magnetometer (VSM, Lakeshore-7304) at 300 K. Thermogravimetric analysis (TGA) was performed on a thermogravimetric analyzer (METTLER SDTA851) from 30 to 800 °C at a heating rate of 10 °C min^{-1} under a N_2 atmosphere. The specific surface areas and pore sizes were determined by a Micromeritics ASAP 2460 analyzer and calculated by the Brunauer–Emmett–Teller (BET) equation and the Barrett–Joyner–Halenda (BJH) adsorption method, respectively.

Mimic Peroxidase Activity of mZIF-8. The mimic peroxidase activity of mZIF-8 was measured as follows: 5 mg of mZIF-8 was dispersed in 1 mL of NaA_C buffer (0.2 M, pH 4.0) and added into the aqueous solution (4 mL) containing OPD (1 mL, 1 mM) and different H_2O_2 concentrations (4.0–316.8 μM). The reaction solution was incubated at room temperature for 10 min in the dark and then separated by an external magnet to remove the mZIF-8 nanoparticles. The absorbance of the obtained solution was examined immediately by a UV–vis spectrophotometer (UNICO-4802, China) at 450 nm to determine the produced DAP concentration. Kinetic parameters (K_m and V_{max}) were calculated by Lineweaver–Burk plots of the Michaelis–Menten equation from three independent tests.

https://doi.org/10.1021/acsami.1c11815
ACS Appl. Mater. Interfaces 2021, 13, 44329–44338

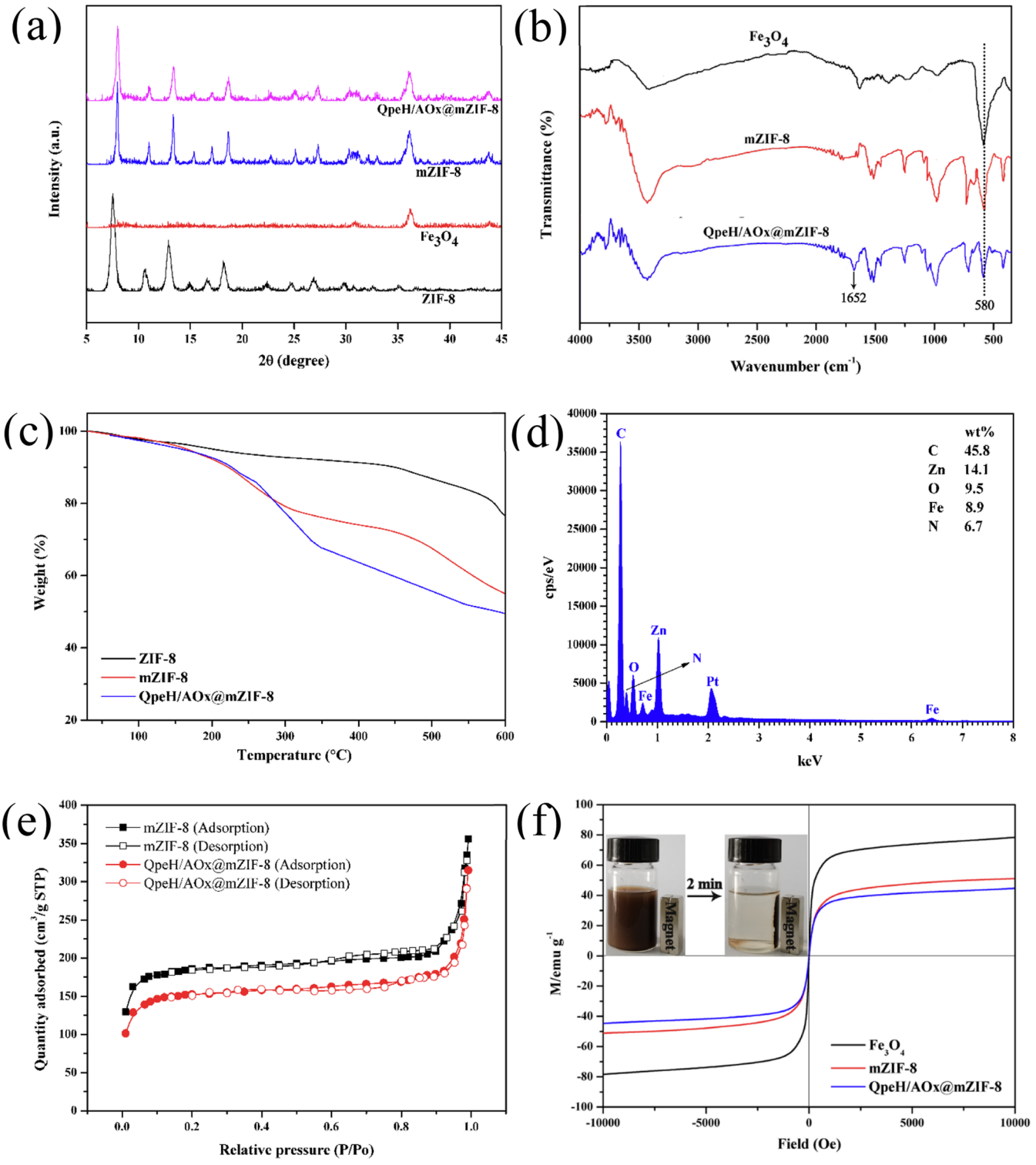

Figure 2. (a) XRD patterns of ZIF-8, Fe_3O_4, mZIF-8, and QpeH/AOx@mZIF-8; (b) FT-IR spectra of Fe_3O_4, mZIF-8, and QpeH/AOx@mZIF-8; (c) TGA curves of ZIF-8, mZIF-8, and QpeH/AOx@mZIF-8; (d) EDS analysis of QpeH/AOx@mZIF-8; (e) N_2 sorption−desorption isotherms of mZIF-8 and QpeH/AOx@mZIF-8; and (f) magnetic hysteresis loops of Fe_3O_4, mZIF-8, and QpeH/AOx@mZIF-8. The inset photograph indicates the magnetic separation of QpeH/AOx@mZIF-8 by an external magnet.

Detection of Quizalofop-P-Ethyl by QpeH/AOx@mZIF-8. Quizalofop-P-ethyl (QpE) was used as a model analyte of AOPP herbicides to determine the biosensor performance of QpeH/AOx@mZIF-8. QpeH/AOx@mZIF-8 (5 mg) dispersed in 1 mL of NaA_C buffer (0.2 M, pH 4.0) was added to the reaction solution (4 mL) containing OPD (1 mL, 1 mM) and various QpE concentrations, followed by incubation at room temperature for 10 min in the dark. Later, the absorbance at 450 nm was recorded after the removal of QpeH/AOx@mZIF-8. Alcohol detection by AOx@mZIF-8 was performed using ethanol as substrates according to the above procedure.

Colorimetric Assay for Environmental Samples. The industrial wastewater was collected from the wastewater treatment facility of an AOPP herbicide QpE plant in the city of Wuhan, China.

https://doi.org/10.1021/acsami.1c11815
ACS Appl. Mater. Interfaces 2021, 13, 44329−44338

Surface soils (10 g, 0−20 cm) from a watermelon field long-term contaminated by QpE were dispersed in 100 mL of DI water for 15 min. The wastewater and soil suspension samples were centrifuged at 12,000 rpm for 10 min before measurement. Later, the supernatant was continuously diluted 10-fold by DI water and reacted with QpeH/AOx@mZIF-8 in NaA_C buffer (0.2 M, pH 4.0) and OPD for 10 min away from light, followed by UV−vis spectrophotometer detection. Meanwhile, QpE quantification from the wastewater and soil suspension was verified by HPLC as described previously.[27]

Detection of Various AOPP Herbicides by QpeH/AOx@mZIF-8. The composite (5 mg) dispersed in NaA_C buffer (0.2 M, pH 4.0) was added into the reaction solution in the presence of OPD (1 mL, 1 mM) and different concentrations of fenoxaprop-P-ethyl (FpE) or haloxyfop-P-methyl (HpE) to evaluate the detection of various herbicides by QpeH/AOx@mZIF-8. The total reaction volume was 5 mL. The concentrations of various analytes were determined at 450 nm absorbance following incubation for 10 min in the dark and QpeH/AOx@mZIF-8 separation by a magnet.

RESULTS AND DISCUSSION

Preparation and Characterization of QpeH/AOx@mZIF-8. The mimic multi-enzyme@mZIF-8 composite was prepared under mild conditions using the rapid self-assembly of Zn^{2+} and HmIm ligands induced by Fe_3O_4 nanoparticles and spontaneous encapsulation of a cascade enzyme system consisting of QpeH and AOx (Scheme 1). The facile one-pot synthesis approach affords enzyme immobilization within 30 min, unlike the formation of organic−inorganic hybrid nanoflowers requiring slow crystallization in 3 days.[30] It also protects the embedded enzymes from adverse conditions and prevents biomolecules from leaching. Here, QpeH/AOx@mZIF-8 was conveniently recovered after a catalytic reaction mediated by an external magnet for the next catalyst owing to the introduction of Fe_3O_4 MNPs. Notably, the three-step cascade reaction is accomplished in a single hybrid composite utilizing hydrolase QpeH, oxidase AOx, and mimic peroxidase of mZIF-8 to form a colored product for AOPP herbicide detection. In this reaction, the intermediates migrate directly to the catalytic site of the downstream enzyme to avoid their decomposition and diffusion hindrance.

The CA-Fe_3O_4 MNPs were prepared by a modified solvothermal reaction as described by Hou *et al.*[28] The SEM image of CA-Fe_3O_4 illustrated in Figure 1a indicates the formation of spherical MNPs with an average diameter of around 25.6 nm (Figure 1c), which was consistent with the particle size of MNPs synthesized by Ricco using atomic force microscopy (AFM) measurements.[26] The SEM images of mZIF-8 and QpeH/AOx@mZIF-8 demonstrated that the composites had the same truncated rhombic dodecahedral morphology with a mean diameter of about 494.5 nm and a rough surface (Figure 1b,d). Compared to HRP/MNP@ZIF-8 prepared through a similar co-precipitation method, the particle sizes of these two composites were smaller. The reason might be because the sustained growth of HRP/MNP@ZIF-8 for another 16 h leads to increased particle size.[31]

The XRD patterns of mZIF-8 and QpeH/AOx@mZIF-8 illustrated in Figure 2a exhibit all diffraction peaks typical of magnetite (JCPDS card no. 19-0629) Fe_3O_4 and ZIF-8 crystal,[32] suggesting no significant effect of MNP and enzyme incorporation on the crystal structure and crystallinity of ZIF-8. The FT-IR spectra illustrated in Figure 2b suggest that the characteristic peaks at 1640−1660 cm^{-1} were assigned to the C═O stretching vibrations of the amide I band,[22] and the enzyme protein was embedded in ZIF-8. The characteristic peak at 580 cm^{-1} was ascribed to the stretching mode of Fe−O,[33] which verified the presence of Fe_3O_4 MNPs in the composites. The TGA profiles of mZIF-8 and QpeH/AOx@mZIF-8 illustrated in Figure 2c indicate less than 7% weight loss below 200 °C due to the evaporation of residual water and solvent from the cavities. The second weight loss of mZIF-8 and QpeH/AOx@mZIF-8 was approximately 11 and 19% between 250 and 350 °C, attributing to the decomposition of MNPs and enzyme protein in ZIF.[34] Compared to the weight loss of the two composites, the loading capacity and loading ratio of enzyme protein inside mZIF-8 were 8 and 86.6%, respectively. The lower enzyme loading capacity and loading ratio of QpeH/AOx@mZIF-8 with respect to catalase@ZIF-8 (12%)[35] with rhombic dodecahedral morphology might be explained by the presence of the competition between the enzyme and MNPs as heterogeneous nucleation seeds. Additionally, the EDS elemental mapping indicated the peaks of the elements C, O, N, Zn, and Fe throughout QpeH/AOx@mZIF-8 (Figures 2d and S1), in which Fe appearance could be assigned to Fe_3O_4 MNP encapsulation within the composite.

The porosity characteristics of mZIF-8 and QpeH/AOx@mZIF-8 were measured by an N_2 sorption−desorption isotherm at 77 K (Figure 2e). The results exhibited a typical type I adsorption−desorption behavior for microporous structure. The BET surface areas of mZIF-8 and QpeH/AOx@mZIF-8 were 611.8 and 526.2 $m^2\ g^{-1}$, respectively. In contrast, QpeH/AOx@mZIF-8 (15.2 nm) had a larger pore size than mZIF-8 (12.6 nm). The porous features of QpeH/AOx@mZIF-8 suggest that the introductions of magnetic content and multi-enzyme do not interfere with the microporous structure of ZIF crystal. Moreover, the large surface area and pore size enable the target analyte to easily cross through the ZIF shell to interact with the enzymes.[36] The magnetic hysteresis loops of Fe_3O_4, mZIF-8, and QpeH/AOx@mZIF-8 were investigated by VSM. As depicted in Figure 2f, the saturation magnetization (Ms) values were 78.3 emu g^{-1} for Fe_3O_4, 51.1 emu g^{-1} for mZIF-8, and 44.7 emu g^{-1} for QpeH/AOx@mZIF-8, respectively. Although QpeH/AOx@mZIF-8 had a decreased Ms value due to the presence of ZIF shell and enzyme molecules on MNP seed surface, QpeH/AOx@mZIF-8 was suitable for simple magnetic separation by an external magnetic field. The inset photograph of Figure 2f demonstrates that a magnet could readily separate QpeH/AOx@mZIF-8 from a liquid suspension in 2 min. Besides, the absence of remanence and coercivity with no hysteresis expressed a superparamagnetic behavior of the prepared magnetic composites at room temperature,[37] suggesting that these composites could be re-dispersed immediately after the removal of the magnet. The above results elucidate that QpeH/AOx@mZIF-8 is suitable for AOPP detection with excellent recyclability and reusability in practical application.

Determination of the Peroxidase-like Activity of mZIF-8. Since the chromogenic reaction using mZIF-8 oxidizing OPD is critical for colorimetric detection of AOPP herbicides based on the QpeH/AOx@mZIF-8 mimic multi-enzyme system, the mimic peroxidase activity of mZIF-8 was first evaluated by measuring the absorbance at 450 nm using OPD as a substrate. As illustrated in Scheme 1, mZIF-8 catalyzed the oxidization of OPD to form orange-colored DAP in the presence of H_2O_2. In a typical experiment, the absorbance at 450 nm was monitored in 10 min after incubation of mZIF-8 in 5 mL of NaA_C buffer (0.2 M, pH 4.0) containing 118.8 μM H_2O_2 and 1 mM OPD at room

https://doi.org/10.1021/acsami.1c11815
ACS Appl. Mater. Interfaces 2021, 13, 44329−44338

temperature. With the increase of the reaction time, the absorbance increased gradually. Finally, a value limit (A_{450} = 0.36) could be achieved at 7 min (Figure S2a). Furthermore, the effects of temperature and pH on the peroxidase-like activity of mZIF-8 were examined. mZIF-8 exhibited high activity at 20−80 °C and an optimum at 50 °C (Figure S2b). The optimal pH of mZIF-8 at room temperature was pH 4.0 (Figure S2c). Although this pH was significantly lower than the optimal pH of free QpeH (pH 8.0)[27] and AOx (pH 7.5), the encapsulation of enzyme in ZIF-8 was confirmed to substantially improve the pH stability due to the effective protection of ZIF-8 scaffold preventing the conformational changes of the embedded enzyme,[38] which allowed QpeH/AOx@mZIF-8 to efficiently execute cascade enzymatic reaction at pH 4.0. Under optimal conditions, an excellent linear relationship between the absorbance and H_2O_2 concentration within the range of 4.0−158.4 μM was observed (R^2 = 0.9962) (Figure 3). This result suggested that excess

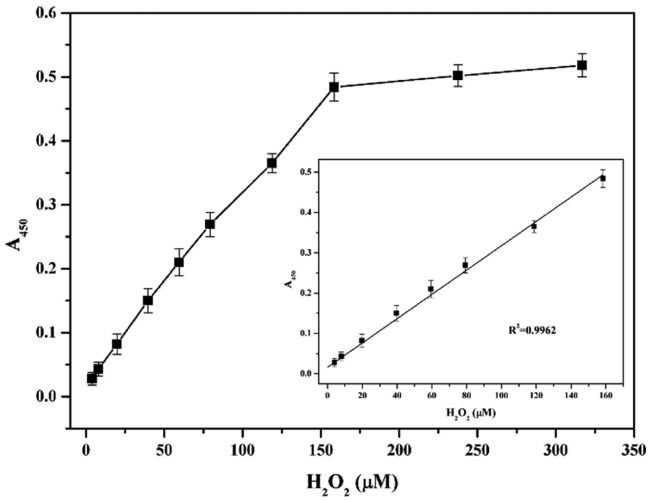

Figure 3. Absorbance at 450 nm of OPD oxidized by mZIF-8 using H_2O_2 in the concentration of 4.0−316.8 μM. The inset photograph indicates the corresponding fitted linear plot.

H_2O_2 production through the cascade catalysis of QpeH and AOx embedded in the QpeH/AOx@mZIF-8 biosensor had no remarkable effect on the absorbance of OPD-H_2O_2 colorimetric reaction.[39] The steady-state kinetic experiments were performed by diluting OPD and H_2O_2 to six different concentrations. When the amount of H_2O_2 in the reaction was excess, the kinetic values K_m and V_{max} of mZIF-8 for OPD were 0.68 mM and 4.28 × 10^{-8} M s^{-1}, respectively. When the reaction was performed with an excess amount of OPD, the K_m value of mZIF-8 for H_2O_2 was 1.18 mM and the V_{max} value was 2.65 × 10^{-8} M s^{-1}. The decreased K_m value of mZIF-8 regardless of OPD or H_2O_2 compared to the free HRP[25,40] demonstrates that the prepared mZIF-8 possesses a higher peroxidase-like activity toward each substrate.

To rule out the possibility that the leached ferrous ions utilized their intrinsic peroxidase-like activity to catalyze the oxidation of OPD, the Fe^{2+} ion concentrations leached from 5 mg of mZIF-8 in 1 mL of NaA_c buffer (0.2 M, pH 4.0) for 20 min were investigated based on the coloration reaction between Fe^{2+} and 1,10-phenanthroline.[41] As displayed in Figure S3a, the amount of Fe^{2+} ions leached from mZIF-8 was almost ignored according to the absorbance at 508 nm. Meanwhile, the structural integrity of mZIF-8 was observed by SEM after the acid treatment with no distinct difference in the morphology before and after treatment (Figure S3b,c). The above results confirm that mZIF-8 has excellent stability under acidic conditions, suggesting that Fe_3O_4 nanoparticles have no significant impact on the peroxidase-like activity of mZIF-8.

Performance Evaluation of AOPP Herbicide Biosensor. The cascade reaction of QpeH/AOx@mZIF-8 resulted in the oxidation of alcohols to H_2O_2 intermediate using oxygen as an electron acceptor. Then, mZIF-8 catalyzed OPD with H_2O_2 to form DAP, which was monitored by a spectrophotometer. Based on this catalytic principle, QpeH/AOx@mZIF-8 as a colorimetric biosensor was found to be suitable for rapid sensing of AOPP herbicides. In a typical detection of the AOPP herbicide QpE, the absorbance at 450 nm was measured 10 min after the incubation of QpE, QpeH/AOx@mZIF-8, and OPD in 5 mL of the reaction solution at room temperature. As depicted in Figure 4a,b, the developed biosensor offered a good linearity of 6.7−214.6 (R^2 = 0.9912) between the absorbance and concentration of the AOPP herbicide QpE and a clear color change was observed (Figure 4a, inset). The limit of detection (LOD) was 8.2 μM according to the equation: LOD = 3σ/S, where σ represents the standard deviation of the biosensor response value with regard to the blank (0.003) and S is the slope value of the calibration curve (0.0011). The LOD of this biosensor is comparable or better than those of the previously reported enzymatic monitoring system based on the colorimetric method for organic pollutants (Table 1). Most importantly, the QpeH/AOx@mZIF-8 mimic multi-enzyme system is simple, rapid, and cost-effective for detecting a complicated AOPP herbicide QpE over a wide range of concentrations.

The applicability of QpeH/AOx@mZIF-8 in determining the AOPP herbicide residues in industrial wastewater from a QpE plant and the surface soils from a watermelon field was verified using the composite. As summarized in Table 2, though the results obtained from the QpeH/AOx@mZIF-8 biosensor were slightly higher than the corresponding validations from standard HPLC analysis, both data were well matched. AOx@mZIF-8 with the capability of alcohol detection was utilized to determine the amount of alcohol and verify whether the alcohol residues caused higher results of QpeH/AOx@mZIF-8 in the tested samples. The absorbance (at 450 nm) of the reaction solutions obtained from the wastewater and soil samples was negligible (data not shown), suggesting that the decreased value of HPLC validations might be the reason for the small loss of the target analyte during the samples pre-preparation, such as extraction and repeated dissolution. Meanwhile, these results suggested that mZIF-8 as a scaffold protected the embedded multi-enzyme's catalytic activity from adverse conditions.[31] Thus, the cascade catalysis of QpeH/AOx@mZIF-8 toward QpE was not significantly affected in the wastewater and soil suspension, suggesting the high specificity of the present multi-enzyme system toward QpE.

The hydrolase QpeH from *Pseudomonas* sp. J-2 exhibited high catalytic activity against six AOPP herbicides, especially QpE, QpT, FpE, and HpE.[27] Since one of the corresponding hydrolytic products of FpE and HpE catalyzed by QpeH were ethanol and methanol, which could be subsequently oxidized by AOx to form H_2O_2, the potential of QpeH/AOx@mZIF-8 as a biosensor in determining FpE and HpE was also evaluated. As depicted in Figure 4c,d, good linearity and sensitivity were

https://doi.org/10.1021/acsami.1c11815
ACS Appl. Mater. Interfaces 2021, 13, 44329−44338

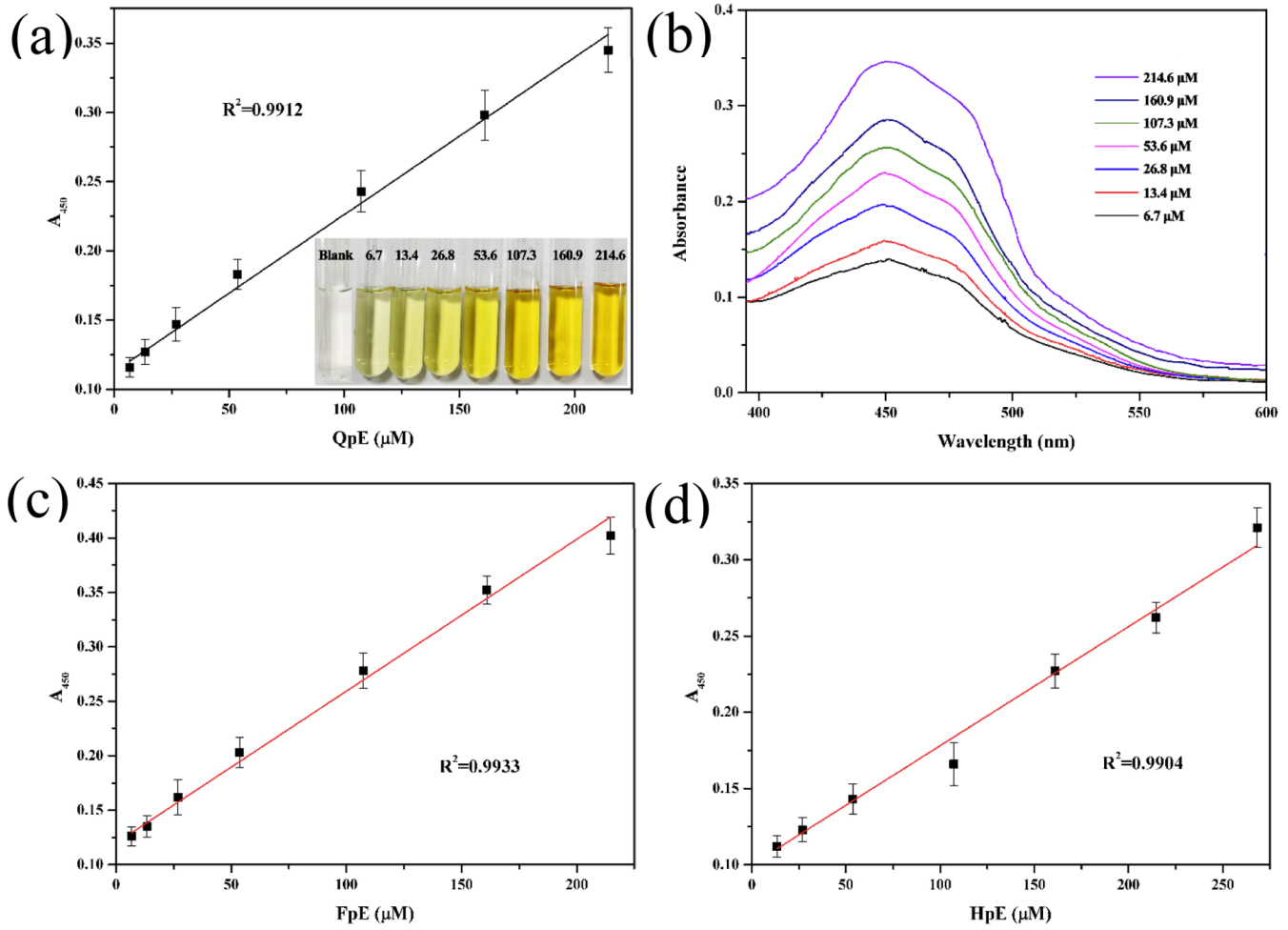

Figure 4. (a) Detection of AOPP herbicide QpE at concentrations of 6.7−214.6 μM by QpeH/AOx@mZIF-8. The inset photograph indicates colorimetric detection of QpE; (b) UV−vis absorption spectra of OPD solutions 10 min after incubation of QpeH/AOx@mZIF-8 with different concentrations of QpE; detection of AOPP herbicides (c) FpE at concentrations of 6.7−214.6 μM and (d) HpE at concentrations of 13.4−268.2 μM by QpeH/AOx@mZIF-8.

Table 1. Comparison of Various Enzymatic Biosensors for the Detection of Organic Pollutants

materials	Pollutants	LOD	dynamic range	stability	reference
Sol−gel-immobilized alkaline phosphatase	metam-sodium	36.5 μM	75.0−480.0 μM		42
	tetradifon	4.9 μM	3.5−28.0 μM		
Ni^{2+}-modified nitrilotriacetic acid agarose	methyl parathion	3.8 μM	1.0−100.0 μM		43
Tb-BTC	methyl parathion	2.6 nM	0.1−1000.0 μM	60 days	20
HRP-MWNTs-GC	2,4-dichlorophenol	0.4 μM	1.0−100.0 μM	14 days	44
$Cu_3(BTC)_2$	2,4-dichlorophenol	9.0 nM	40.0−1000.0 nM		45
Cu-MOF-GN/GCE	hydroquinone	0.6 μM	1.0−1000.0 μM		46
	catechol	0.3 μM			
SiSG-TYR/Fe_3O_4-MWCNTs/GCE	hydroquinone	57.0 nM	1.5−40.0 μM	14 days	47
	catechol	55.0 nM	1.5−30.0 μM		
Cu-MOF/rGO	nitrite	33.0 nM	3.0−40000.0 μM		48
QpeH/AOx@mZIF-8	QpE	8.2 μM	8.2−214.6 μM	50 days	this work
	FpE	6.7 μM	6.7−214.6 μM		
	HpE	13.4 μM	13.4−268.2 μM		

observed in a broad range of 6.7−214.6 μM for FpE and 13.4−268.2 μM for HpE. This demonstrates that the QpeH/AOx@mZIF-8 system is a multifunctional colorimetric biosensor rapidly achieving the visible detection of various AOPP herbicides.

Stability and Reusability of QpeH/AOx@mZIF-8. The long-term storage stability of biosensors is an essential aspect to extend the application and reduce the usage costs. To investigate the stability of the multi-enzyme system, the QpeH/AOx@mZIF-8 composite was sealed, stored at 4 °C for 60 days, and the absorbance at 450 nm was measured 10 min after the incubation of reaction solution containing QpeH/AOx@mZIF-8, OPD, and QpE at room temperature. As depicted in Figure S4a, QpeH/AOx@mZIF-8 retained above

https://doi.org/10.1021/acsami.1c11815
ACS Appl. Mater. Interfaces 2021, 13, 44329−44338

Table 2. Application of QpeH/AOx@mZIF-8 for the Detection of AOPP Herbicide QpE Residues in Real Environmental Samples

samples	dilution factor	absorbance at 450 nm	tested concentrations (μM)	HPLC validations (μM)
industrial wastewater	1	0.334 ± 0.028		1110.2 ± 123.4
	10	0.271 ± 0.022	121.6 ± 8.7	112.5 ± 13.5
	100	0.126 ± 0.018	11.6 ± 1.4	10.7 ± 2.4
surface soils	1	0.133 ± 0.024	17.8 ± 2.7	16.1 ± 3.6
	10	0.113 ± 0.016		1.6 ± 0.3

90% of the initial activity for at least 50 days with good stability. The MNP utilization facilitates the reuse of immobilized multi-enzyme systems. To assess the reusability of QpeH/AOx@mZIF-8 as a biosensor, the magnetic nanoparticles were separated by a magnet and washed with phosphate-buffered solution (50 mM, pH 7.5) after each catalysis. Later, this solution was re-used in the next reaction to detect the absorbance of the supernatant after centrifugation. As depicted in Figure S4b, QpeH/AOx@mZIF-8 displayed excellent reusability over 12 cycles. The residues activity showed no significant decrease for five cycles and reached 85% of the initial activity even after 12 times reuse. Notably, a decline in the catalytic activity might be partially attributed to the loss of QpeH/AOx@mZIF-8 during the repeated separation. The above results suggest that mZIF-8 as a promising support for enzyme immobilization could largely improve the practical utility of QpeH/AOx@mZIF-8 for AOPP herbicide detection.

CONCLUSIONS

In conclusion, a magnetic ZIF-8-based mimic multi-enzyme system as a colorimetric biosensor was developed for AOPP herbicide detection. The prepared QpeH/AOx@mZIF-8 composite showed a fascinating mimetic peroxidase activity of nanozyme MNPs and simultaneously possessed AOPP herbicide hydrolase and alcohol oxidase properties. The cascade enzymatic reaction combined with QpeH/AOx@mZIF-8 effectively avoided the diffusion hindrance and decomposition of intermediates allowing rapid, sensitive, and one-step assay of AOPP herbicides. The colorimetric biosensor exhibited a wide detection range of AOPP herbicides QpE, FpE, and HpE and a comparable or better limit of QpE detection than the previously reported enzymatic biosensors. The quantitative assay of QpE residues in the industrial wastewater and field soils suggested that QpeH/AOx@mZIF-8 was potential enough for simple and reliable detection of AOPP herbicide in real environmental samples. Furthermore, the long-term storage stability, easy separation, and reusability of QpeH/AOx@mZIF-8 make it promising for developing low-cost and robust AOPP herbicide biosensors. This study will provide insights into the development of an enzymatic biosensor for rapid detection of the complex environmental contaminants.

ASSOCIATED CONTENT

Supporting Information

The Supporting Information is available free of charge at https://pubs.acs.org/doi/10.1021/acsami.1c11815.

SEM image of QpeH/AOx@mZIF-8 and EDS elemental mappings of C, Zn, O, N, and Fe; effects of time, temperature, and pH on the mimic peroxidase activity of mZIF-8; UV−vis absorption spectra of Fe_3O_4 and mZIF-8 via the coloration reaction between Fe^{2+} and 1,10-phenanthroline at pH 4.0; SEM images of mZIF-8 before and after the acid treatment at pH 4.0; and storage stability and reusability of QpeH/AOx@mZIF-8 (PDF)

AUTHOR INFORMATION

Corresponding Authors

Hui Zhang − *College of Life Sciences, Huaibei Normal University, Huaibei 235000, China;* orcid.org/0000-0001-6410-4085; Email: guzhang503@sina.cn

Feng Li − *College of Life Sciences, Huaibei Normal University, Huaibei 235000, China*; Phone: +86 561 3803024; Email: lfgrx@sohu.com

Authors

Hengyan Ma − *College of Life Sciences, Huaibei Normal University, Huaibei 235000, China*

Mengya Li − *College of Life Sciences, Huaibei Normal University, Huaibei 235000, China*

Ting Yu − *College of Life Sciences, Huaibei Normal University, Huaibei 235000, China*

Minghua Xiong − *College of Life Sciences, Huaibei Normal University, Huaibei 235000, China*

Complete contact information is available at: https://pubs.acs.org/10.1021/acsami.1c11815

Notes

The authors declare no competing financial interest.

ACKNOWLEDGMENTS

This work was supported by the Natural Science Foundation of Anhui Province (1808085MC56), the University Synergy Innovation Program of Anhui Province (GXXT-2019-034), the Innovation Team of Scientific Research Platform of Anhui Province, China (KJ2015TD001), and Anhui Province Key Laboratory of Pollutant Sensitive Materials and Environmental Remediation.

REFERENCES

(1) Yan, Z.; Yang, Z.; Deng, X.; Lin, D.; Wu, M.; Li, J.; Chen, A.; Ye, J.; Hu, A.; Liao, H. Novel Aryloxyphenoxypropionate Derivates Containing Benzofuran Moiety: Design, Synthesis, Herbicidal Activity, Docking Study and Theoretical Calculation. *Pestic. Biochem. Physiol.* **2019**, *154*, 78−87.

(2) Busi, R.; Goggin, D. E.; Heap, I. M.; Horak, M. J.; Jugulam, M.; Masters, R. A.; Napier, R. M.; Riar, D. S.; Satchivi, N. M.; Torra, J.; Westra, P.; Wright, T. R. Weed Resistance to Synthetic Auxin Herbicides. *Pest Manag. Sci.* **2018**, *74*, 2265−2276.

(3) Zhou, J.; Liu, K.; Xin, F.; Ma, J.; Xu, N.; Zhang, W.; Fang, Y.; Jiang, M.; Dong, W. Recent Insights into the Microbial Catabolism of Aryloxyphenoxy-Propionate Herbicides: Microbial Resources, Metabolic Pathways and Catabolic Enzymes. *World J. Microbiol. Biotechnol.* **2018**, *34*, 117.

(4) Markets and markets. Herbicides Market by Type (Glyphosate, 2, 4-D, Diquat), Crop Type (Cereals & Grains, Oilseeds & Pulses, Fruits & Vegetables), Mode of Action (Non-selective, Selective), and Region−Global Forecast to. 2020, 2022. https://www.marketsandmarkets.com/Market-Reports/herbicides-357.html.accessed 2021-02-12.
(5) Huang, X.; He, J.; Yan, X.; Hong, Q.; Chen, K.; He, Q.; Zhang, L.; Liu, X.; Chuang, S.; Li, S.; Jiang, J. Microbial Catabolism of Chemical Herbicides: Microbial Resources, Metabolic Pathways and Catabolic Genes. *Pestic. Biochem. Physiol.* **2017**, *143*, 272−297.
(6) López-Ruiz, R.; Romero-González, R.; Martínez Vidal, J. L.; Garrido Frenich, A. Behavior of quizalofop-p and its commercial products in water by liquid chromatography coupled to high resolution mass spectrometry. *Ecotoxicol. Environ. Saf.* **2018**, *157*, 285−291.
(7) Yin, X.; Li, S.; Liu, S.; Zhu, G.; Zhuang, H. Genotoxicity Evaluation of Low Doses of Clodinafop-Propargyl to the Silkworm Bombyx Mori Using Alkaline Single-Cell Gel Electrophoresis. *Environ. Toxicol. Pharmacol.* **2008**, *26*, 162−166.
(8) Elefsiniotis, I. S.; Liatsos, G. D.; Stamelakis, D.; Moulakakis, A. Case Report: Mixed Cholestatic/Hepatocellular Liver Injury Induced by the Herbicide Quizalofop-p-Ethyl. *Environ. Health Perspect.* **2007**, *115*, 1479−1481.
(9) Rosculete, C.; Bonciu, E.; Rosculete, E.; Olaru, L. Determination of the Environmental Pollution Potential of Some Herbicides by the Assessment of Cytotoxic and Genotoxic Effects on Allium cepa. *Int. J. Environ. Res. Publ. Health* **2018**, *16*, 75.
(10) Aksoy, O.; Dane, F.; Ekinci Sanal, F.; Aktac, T. The Effects of Fusilade (Fluazifop-p-Butyl) on Germination, Mitotic Frequency and α-Amylase Activity of Lentil (Lens Culinaris Medik.) Seeds. *Acta Physiol. Plant.* **2007**, *29*, 115−120.
(11) Wu, J.; Wang, K.; Zhang, Y.; Zhang, H. Determination and Study on Dissipation and Residue Determination of Cyhalofop-Butyl and Its Metabolite Using HPLC-MS/MS in a Rice Ecosystem. *Environ. Monit. Assess.* **2014**, *186*, 6959−6967.
(12) Farajzadeh, M. A.; Mohebbi, A.; Feriduni, B. Development of Continuous Dispersive Liquid-Liquid Microextraction Performed in Home-Made Device for Extraction and Preconcentration of Aryloxyphenoxy-Propionate Herbicides from Aqueous Samples Followed by Gas Chromatography-Flame Ionization Detection. *Anal. Chim. Acta* **2016**, *920*, 1−9.
(13) Uniyal, S.; Sharma, R. K. Technological Advancement in Electrochemical Biosensor Based Detection of Organophosphate Pesticide Chlorpyrifos in the Environment: A Review of Status and Prospects. *Biosens. Bioelectron.* **2018**, *116*, 37−50.
(14) Prabhakar, N.; Arora, K.; Singh, S. P.; Singh, H.; Malhotra, B. D. DNA Entrapped Polypyrrole-Polyvinyl Sulfonate Film for Application to Electrochemical Biosensor. *Anal. Biochem.* **2007**, *366*, 71−79.
(15) Talan, A.; Mishra, A.; Eremin, S. A.; Narang, J.; Kumar, A.; Gandhi, S. Ultrasensitive Electrochemical Immuno-Sensing Platform Based on Gold Nanoparticles Triggering Chlorpyrifos Detection in Fruits and Vegetables. *Biosens. Bioelectron.* **2018**, *105*, 14−21.
(16) Yi, J.; Liu, Z.; Liu, J.; Liu, H.; Xia, F.; Tian, D.; Zhou, C. A Label-Free Electrochemical Aptasensor Based on 3D Porous CS/Rgo/GCE for Acetamiprid Residue Detection. *Biosens. Bioelectron.* **2020**, *148*, 111827.
(17) Nadar, S. S.; Rathod, V. K. Magnetic-Metal Organic Framework (Magnetic-MOF): A Novel Platform for Enzyme Immobilization and Nanozyme Applications. *Int. J. Biol. Macromol.* **2018**, *120*, 2293−2302.
(18) Lyu, F.; Zhang, Y.; Zare, R. N.; Ge, J.; Liu, Z. One-Pot Synthesis of Protein-Embedded Metal-Organic Frameworks with Enhanced Biological Activities. *Nano Lett.* **2014**, *14*, 5761−5765.
(19) Mehta, J.; Dhaka, S.; Paul, A. K.; Dayananda, S.; Deep, A. Organophosphate Hydrolase Conjugated Uio-66-NH(2) MOF Based Highly Sensitive Optical Detection of Methyl Parathion. *Environ. Res.* **2019**, *174*, 46−53.
(20) Mehta, J.; Dhaka, S.; Bhardwaj, N.; Paul, A. K.; Dayananda, S.; Lee, S. E.; Kim, K. H.; Deep, A. Application of an Enzyme Encapsulated Metal-Organic Framework Composite for Convenient Sensing and Degradation of Parathion. *Sens. Actuators, B* **2019**, *290*, 267−274.
(21) Wu, X.; Ge, J.; Yang, C.; Hou, M.; Liu, Z. Facile Synthesis of Multiple Enzyme-Containing Metal-Organic Frameworks in a Biomolecule-Friendly Environment. *Chem. Commun.* **2015**, *51*, 13408−13411.
(22) Wu, X.; Yang, C.; Ge, J. Green Synthesis of Enzyme/Metal-Organic Framework Composites with High Stability in Protein Denaturing Solvents. *Bioresour. Bioprocess.* **2017**, *4*, 24.
(23) Bagheri, N.; Khataee, A.; Hassanzadeh, J.; Habibi, B. Sensitive Biosensing of Organophosphate Pesticides Using Enzyme Mimics of Magnetic ZIF-8. *Spectrochim. Acta, Part A* **2019**, *209*, 118−125.
(24) Gannavarapu, K. P.; Ganesh, V.; Thakkar, M.; Mitra, S.; Dandamudi, R. B. Nanostructured Diatom-ZrO(2) Composite as a Selective and Highly Sensitive Enzyme Free Electrochemical Sensor for Detection of Methyl Parathion. *Sens. Actuators, B* **2019**, *288*, 611−617.
(25) Hou, C.; Wang, Y.; Ding, Q.; Jiang, L.; Li, M.; Zhu, W.; Pan, D.; Zhu, H.; Liu, M. Facile Synthesis of Enzyme-Embedded Magnetic Metal-Organic Frameworks as a Reusable Mimic Multi-Enzyme System: Mimetic Peroxidase Properties and Colorimetric Sensor. *Nanoscale* **2015**, *7*, 18770−18779.
(26) Ricco, R.; Wied, P.; Nidetzky, B.; Amenitsch, H.; Falcaro, P. Magnetically Responsive Horseradish Peroxidase@ZIF-8 for Biocatalysis. *Chem. Commun.* **2020**, *56*, 5775−5778.
(27) Zhang, H.; Li, M.; Li, J.; Wang, G.; Liu, Y. Purification and Properties of a Novel Quizalofop-p-Ethyl-Hydrolyzing Esterase Involved in Quizalofop-p-Ethyl Degradation by Pseudomonas sp. J-2. *Microb. Cell Factories* **2017**, *16*, 80.
(28) Hou, C.; Wang, Y.; Zhu, H.; Zhou, L. Formulation of Robust Organic-Inorganic Hybrid Magnetic Microcapsules through Hard-Template Mediated Method for Efficient Enzyme Immobilization. *J. Mater. Chem. B* **2015**, *3*, 2883−2891.
(29) He, H.; Han, H.; Shi, H.; Tian, Y.; Sun, F.; Song, Y.; Li, Q.; Zhu, G. Construction of Thermophilic Lipase-Embedded Metal-Organic Frameworks via Biomimetic Mineralization: A Biocatalyst for Ester Hydrolysis and Kinetic Resolution. *ACS Appl. Mater. Interfaces* **2016**, *8*, 24517−24524.
(30) Ge, J.; Lei, J.; Zare, R. N. Protein-Inorganic Hybrid Nanoflowers. *Nat. Nanotechnol.* **2012**, *7*, 428−432.
(31) Chen, S.; Wen, L.; Svec, F.; Tan, T.; Lv, Y. Magnetic Metal−Organic Frameworks as Scaffolds for Spatial Co-location and Positional Assembly of Multi-Enzyme Systems Enabling Enhanced Cascade Biocatalysis. *RSC Adv.* **2017**, *7*, 21205−21213.
(32) Park, K. S.; Ni, Z.; Côté, A. P.; Choi, J. Y.; Huang, R.; Uribe-Romo, F. J.; Chae, H. K.; O'Keeffe, M.; Yaghi, O. M. Exceptional chemical and thermal stability of zeolitic imidazolate frameworks. *Proc. Natl. Acad. Sci. U.S.A.* **2006**, *103*, 10186−10191.
(33) Zhao, M.; Zhang, X.; Deng, C. Rational Synthesis of Novel Recyclable Fe_3O_4@MOF Nanocomposites for Enzymatic Digestion. *Chem. Commun.* **2015**, *51*, 8116−8119.
(34) Schejn, A.; Mazet, T.; Falk, V.; Balan, L.; Aranda, L.; Medjahdi, G.; Schneider, R. Fe_3O_4@ZIF-8: Magnetically Recoverable Catalysts by Loading Fe_3O_4 Nanoparticles inside a Zinc Imidazolate Framework. *Dalton Trans.* **2015**, *44*, 10136−10140.
(35) Cui, J.; Feng, Y.; Lin, T.; Tan, Z.; Zhong, C.; Jia, S. Mesoporous Metal-Organic Framework with Well-Defined Cruciate Flower-Like Morphology for Enzyme Immobilization. *ACS Appl. Mater. Interfaces* **2017**, *9*, 10587−10594.
(36) Tian, C.; Zhang, C.; Wu, H.; Song, Y.; Shi, J.; Wang, X.; Song, X.; Yang, C.; Jiang, Z. Merging of Covalent Cross-Linking and Biomimetic Mineralization into an LBL Self-Assembly Process for the Construction of Robust Organic-Inorganic Hybrid Microcapsules. *J. Mater. Chem. B* **2014**, *2*, 4346−4355.

https://doi.org/10.1021/acsami.1c11815
ACS Appl. Mater. Interfaces 2021, 13, 44329−44338

(37) Pang, F.; He, M.; Ge, J. Controlled Synthesis of Fe_3O_4/ZIF-8 Nanoparticles for Magnetically Separable Nanocatalysts. *Chemistry* **2015**, *21*, 6879−6887.
(38) Yu, T.; Ma, H.; Zhang, H.; Xiong, M.; Liu, Y.; Li, F. Fabrication and Characterization of Purified Esterase-Embedded Zeolitic Imidazolate Frameworks for the Removal and Remediation of Herbicide Pollution from Soil. *J. Environ. Manag.* **2021**, *288*, 112450.
(39) Tian, J.; Liu, S.; Luo, Y.; Sun, X. Fe(III)-Based Coordination Polymer Nanoparticles: Peroxidase-Like Catalytic Activity and Their Application to Hydrogen Peroxide and Glucose Detection. *Catal. Sci. Technol.* **2012**, *2*, 432−436.
(40) Gao, L.; Zhuang, J.; Nie, L.; Zhang, J.; Zhang, Y.; Gu, N.; Wang, T.; Feng, J.; Yang, D.; Perrett, S.; Yan, X. Intrinsic Peroxidase-Like Activity of Ferromagnetic Nanoparticles. *Nat. Nanotechnol.* **2007**, *2*, 577−583.
(41) Yang, Q.-Y.; Cheng, C.-Q.; Ruan, F.-P.; Wang, W.-T.; Zhou, Z.-Z.; Wang, D.-Y.; Guan, M.; Meng, X.-M.; Zhao, J. Highly Sensitive Image Recognition on Iron Contamination for 316L Austenitic Stainless Steel by Regent Additives into Color-Change Indicator. *J. Nondestr. Eval.* **2020**, *39*, 19.
(42) Sánchez, F. G.; Díaz, A. N.; Peinado, M. C. R.; Belledone, C. Free and Sol−Gel Immobilized Alkaline Phosphatase-Based Biosensor for the Determination of Pesticides and Inorganic Compounds. *Anal. Chim. Acta* **2003**, *484*, 45−51.
(43) Lan, W.; Chen, G.; Cui, F.; Tan, F.; Liu, R.; Yushupujiang, M. Development of a Novel Optical Biosensor for Detection of Organophoshorus Pesticides Based on Methyl Parathion Hydrolase Immobilized by Metal-Chelate Affinity. *Sensors* **2012**, *12*, 8477−8490.
(44) Huang, S.; Qu, Y.; Li, R.; Shen, J.; Zhu, L. Biosensor Based on Horseradish Peroxidase Modified Carbon Nanotubes for Determination of 2,4-Dichlorophenol. Microchim. *Acta* **2008**, *162*, 261−268.
(45) Dong, S.; Suo, G.; Li, N.; Chen, Z.; Peng, L.; Fu, Y.; Yang, Q.; Huang, T. A Simple Strategy to Fabricate High Sensitive 2,4-Dichlorophenol Electrochemical Sensor Based on Metal Organic Framework $Cu_3(BTC)_2$. *Sens. Actuators, B* **2016**, *222*, 972−979.
(46) Li, J.; Xia, J.; Zhang, F.; Wang, Z.; Liu, Q. An Electrochemical Sensor Based on Copper-Based Metal-Organic Frameworks-Graphene Composites for Determination of Dihydroxybenzene Isomers in Water. *Talanta* **2018**, *181*, 80−86.
(47) Shaikshavali, P.; Madhusudana Reddy, T.; Venu Gopal, T.; Venkataprasad, G.; Narasimha, G.; Lakshmi Narayana, A.; Hussain, O. M. Development of Carbon-Based Nanocomposite Biosensor Platform for the Simultaneous Detection of Catechol and Hydroquinone in Local Tap Water. *J. Mater. Sci.* **2021**, *32*, 5243−5258.
(48) Saraf, M.; Rajak, R.; Mobin, S. M. A Fascinating Multitasking Cu-MOF/Rgo Hybrid for High Performance Supercapacitors and Highly Sensitive and Selective Electrochemical Nitrite Sensors. *J. Mater. Chem. A* **2016**, *4*, 16432−16445.

https://doi.org/10.1021/acsami.1c11815
ACS Appl. Mater. Interfaces 2021, 13, 44329−44338